Journal of Molecular Catalysis A: Chemical 392 (2014) 235–240

Contents lists available at ScienceDirect

Journal of Molecular Catalysis A: Chemical

journal homepage: www.elsevier.com/locate/molcata

Reductive amination of furfural over Me/SiO_2–SO_3H (Me: Pt, Ir, Au) catalysts

José J. Martínez[a,*], Eliana Nope[a], Hugo Rojas[a], María H. Brijaldo[b], Fabio Passos[b], Gustavo Romanelli[c]

[a] Escuela de Ciencias Químicas, Facultad de Ciencias. Universidad Pedagógica y Tecnológica de Colombia UPTC, Avenida Central del Norte, Tunja, Boyacá, Colombia
[b] Departamento de Engenharia Química e de Petróleo, Universidade Federal Fluminense, R. Passos da Pátria, 156, Niterói, RJ 24210-240, Brazil
[c] Centro de Investigación y Desarrollo en Ciencias Aplicadas "Dr. J.J. Ronco" (CINDECA), Departamento de Química, Facultad de Ciencias Exactas, UNLP-CCT-CONICET, Calles 47 No. 257, B1900 AJK La Plata, Argentina

ARTICLE INFO

Article history:
Received 22 March 2014
Received in revised form 17 May 2014
Accepted 19 May 2014
Available online 27 May 2014

Keywords:
Reductive amination
Furfural
Metal colloids
Sulfonated silica

ABSTRACT

Gold, platinum and iridium colloids were supported on sulfonic acid-functionalized silica and were employed for the reductive amination of furfural. The catalysts were characterized by N_2-physisorption at 77 K, X-ray diffraction, H_2 chemisorption and XPS. The results indicated that Ir, Au and Pt colloids were uniformly dispersed on the SiO_2–SO_3H support. XPS results showed the interaction of sulfonic acid groups and metal sites which favors the formation of imine and its subsequent hydrogenation to amine.

1. Introduction

Reductive amination involving the reaction of carbonyl compounds with amines remains one of the most versatile and useful synthetic routes for the synthesis of amines and their derivatives, which are used as synthetic organic intermediates in pharmaceuticals and agrochemicals. The process involves the formation of an imine or iminium intermediate followed by its reduction to amine. Commonly, $NaBH_4$ has been employed with various Brönsted acids for successful reductive amination; however, these acids are corrosive, toxic and difficult to separate from the reaction solution and therefore, it is interesting to substitute them with more environmentally friendly solid acids [1]. Thus, acid solids combined with $NaHB_4$ such as $H_3PW_{12}O_{40}$/$NaBH_4$ [1], $NaBH_4$/wet clay, [2] $NaBH_4$/Brönsted acidic ionic liquid, [3] $NaBH_4$/cellulose sulfuric acid [4], $NaBH_4$/silica-gel-supported sulfuric acid [5], among others, have been used. Recently, Deng et al. [6] using sulfonic acid supported on hydroxyapatite and in the presence of sodium borohydride, reported the preparation of secondary or tertiary amines with high yields, with the advantage of easy separation by applying a magnetic field.

Another approach is direct reductive amination using heterogeneous catalysts, in which both reducing sites such as acid-base sites are necessary [7–10]. The presence of acid sites ensures imine formation. In fact, the presence of Brönsted acid sites significantly increases the amine yield [7], as similarly occurs in $NaBH_4$ supported catalysts. Acid sites significantly increase the reactivity, as has been observed in Pd/C [8,11] and Ru/C catalysts [11] pretreated with $(NH_4)_2S_2O_8$, which favored the acidity of the carbon surface and consequently, the reactivity and selectivity of carbon-supported noble metal catalysts in the reductive amination of benzaldehyde with ammonia. However, the selectivity strongly depends on the metal employed [11] and on the hydrogenation step of imine intermediates [9].

For controlling reaction selectivity in heterogeneous catalysis, it is necessary to prepare catalysts that exhibit only specific types of sites required for desired product formation. Recently, Zhu et al. [12] argued that over Ru/SiO_2–SO_3H catalysts, in the hydrogenation step the substrate molecules might be more easily desorbed from the Ru center due to poisoning/coordination of the sulfonic acid group to the metal center, which avoids further side reactions and inherently favors the catalytic activity. Considering these results, in this work we prepared Au, Ir and Pt colloids stabilized with

* Corresponding author. Tel.: +57 987432800.
E-mail addresses: jose.martinez@uptc.edu.co, jjmartinezz@unal.edu.co (J.J. Martínez).

http://dx.doi.org/10.1016/j.molcata.2014.05.014
1381-1169/

polyvinylpyrrolidine (PVP) deposited over SiO_2 grafted with sulfonic acid. In this bifunctional catalyst, sulfonic acid groups should act as active sites for the first step of acid hydrolysis and as metal nanoparticles for hydrogenation in the second step. The influence of metal sites and the proximate sulfonic acid group through the electron transfer in the bifunctional catalyst should produce an effect on the hydrogenation step.

The reaction of furfural with aniline was chosen as a model reaction for direct reductive amination (Fig. 1). Furfural is an interesting platform molecule due to the high amount of hemicellulose produced by hydrolysis and nowadays seems to be the only unsaturated large-volume organic chemical prepared from carbohydrate sources [13].

Our aim was to demonstrate that the use of a bifunctional catalyst favors the reductive amination of furfural with aniline. The reaction should proceed slowly without the acidic sites; however, the acid/acidic sites should protonate carbonyl group/groups (si fuera solo uno, debería ser 'the carbonyl group'), making carbonylic carbon a better electrophile and activating it more easily toward nucleophilic attacks in the first step, which favors the hydrogenation of imine and consequently, the desired amine formation.

2. Experimental

2.1. Materials and methods

Toluene (Panreac, 99.5%), 3-mercaptopropyltrimethoxysilane (MPTMS) (Sigma–Aldrich, 95%), hydrogen peroxide (H_2O_2) (Panreac, 30%), hydrochloric acid (Sigma–Aldrich, 37%), $FeCl_3{\cdot}6H_2O$ (Sigma–Aldrich, 99%), $FeCl_2{\cdot}3H_2O$ (Sigma–Aldrich, 97%), sodium hydroxide (Panreac, 98%), acetone (Sigma–Aldrich, 99.5%), tetraethylorthosilicate (TEOS) (Sigma–Aldrich, 99%), aluminum isopropoxide (Fluka, 97%), ethanol (Sigma–Aldrich, 99.5%), D-xylose (Sigma–Aldrich), commercial silica and alumina (Syloid and BASF, respectively) were used.

2.2. Catalyst preparation

2.2.1. Synthesis of SiO_2–SO_3H

A mixture of 5 g of SiO_2 (Syloid $S_{BET} = 283\ m^2\ g^{-1}$) or γ-Al_2O_3 (BASF) in 100 mL of dry toluene, and 3-mercaptopropyltrimethoxysilane (MPTMS) (1.15 mL, 6.1 mmol) was refluxed for 24 h. The solid obtained was washed with toluene and dried at 363 K. Subsequently, mercaptopropyl groups were oxidized to sulfonic acid groups with excess hydrogen peroxide at room temperature for 24 h, a few drops of H_2SO_4 were added during 12 h, and the solid was washed with acetone and dried at 393 K. The solids obtained were SiO_2–SO_3H and Al_2O_3–SO_3, respectively.

2.2.2. Synthesis of Me/SiO_2–SO_3H (Me: Au, Ir, Pt)

The synthesis of PVP-Me colloids was similar to that described in the literature [14]. Briefly, 1.11 g PVP and 0.130 g of metal precursor ($HAuCl_4$, H_2IrCl_6 and H_2PtCl_6) were dissolved in a mixed solution of 130 mL methanol and 150 mL water, and then 20 mL 0.1 M NaOH methanol solution was added dropwise with vigorous stirring. The reaction mixture was refluxed to give a color change; a homogeneous black colloidal solution was obtained for Pt and Ir, while for Au a violet colloidal solution was formed.

The colloids were supported on SiO_2–SO_3H with stirring and were maintained at room temperature for 6 h under stirring, then they were dried under vacuum at 353 K.

2.3. Characterization of catalysts

The X-ray diffraction measurements were carried out with a Rigaku Miniflex II using Cu Kα radiation (λ = 1.54056 Å). The XRD patterns were recorded in the 2θ range of 10–90°, using a count time of 1 s and a step size of 0.05°. Crystallite sizes were calculated from the line broadening of the main XRD peaks by using the Debye-Scherrer equation.

Textural properties of the solids were obtained by N_2 adsorption–desorption isotherms measured at 77 K in Micromeritics ASAP 2020 equipment. Samples were previously evacuated at 623 K for 16 h. The BET method was used to calculate the total surface area of the samples.

The metal dispersion of catalysts was evaluated by H_2–O_2 titration using Micromeritics ASAP 2020 apparatus at 308 K. The catalysts were activated under vacuum at 373 K for 2 h, followed by evacuation at 308 K for 60 min. After cooling at 308 K, the catalysts were subjected to a flow of O_2 to form Me–O surface species and then evacuated for 30 min at 308 K for 2 h. Subsequently, H_2 analysis at 308 K was performed. The metal dispersion, surface area, and particle size were determined from the hydrogen uptake isotherm obtained, assuming a H/Me stoichiometry of 1.5.

The sample surfaces were characterized by XPS. Data were obtained from a Thermo Scientific Escalab 250 XI Photoelectron spectrometer. Measurements were performed at room temperature with monochromatic Al Kα radiation ($h\nu$ = 1486.6 eV). The analyzer was operated at 25 eV pass energy and a step size of 0.05 eV. The pressure in the analytical chamber was 6.3×10^{-8} mBar. The signal of C 1s (284.6 eV) was used as internal energy reference. Core-level peak positions were determined after background subtraction using CasaXPS software. Peaks in a spectrum were fitted by a combination of Gaussian and Lorentzian curves, which also allowed separating overlapping peaks.

The acid capacity was determined by titration with 0.01 M NaOH (*aq*) [15]. In a typical experiment, 0.1 g of solid was added to 10 mL of deionized water. The resulting suspension was allowed to equilibrate and thereafter was titrated by dropwise addition of 0.01 M NaOH solution using phenolphthalein as pH indicator.

2.4. Catalytic studies

The liquid phase amination reductive reaction was carried out in a batch-type reactor at a constant stirring rate (1000 rpm) under the following conditions: hydrogen partial pressure, 5 MPa; catalyst sample, 25 mg; 40 mL of a 0.1 M solution of furfural and 0.1 M solution of aniline in distinct solvents, and reaction temperature of 363 K. Reaction products were analyzed in a GC–MS Varian 3800 furnished with a β-Dex column, He as carrier, and constant temperature of 393 K.

3. Results and discussion

3.1. Characterization of catalysts

Table 1 summarizes the textural properties of the solids obtained from the N_2 adsorption–desorption isotherms at 77 K. The solids showed type IV isotherms according to the IUPAC classification (Fig. 2). The impregnation with the metal colloids significantly affected the textural properties, causing a slight decrease in surface area and increasing the pore volume and pore size.

The acid capacity of the samples was determined by titration with 0.01 M NaOH (*aq*). The results in terms of mmol H^+/g of SO_3H groups are listed in Table 2. The impregnation with colloids decreased the acid capacities, possibly due to some interaction of

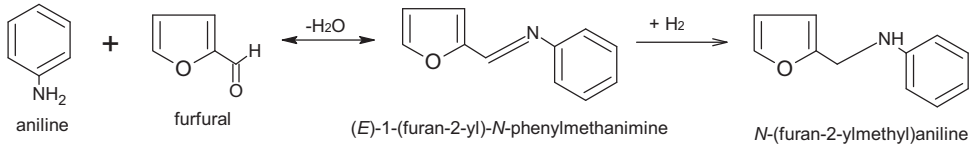

Fig. 1. Reductive amination of furfural with aniline.

Table 1
Textural properties and acid capacities by NaOH titration (mmol H^+/g) of the different solids studied.

Catalyst	S_{BET} ($m^2\ g^{-1}$)	Pore volume ($cm^3\ g^{-1}$)	Pore size (nm)	Acid capacities (mmol H^+/g of SO_3H)
SiO_2–SO_3H	251	0.45	7.2	35.8
Au/SiO_2–SO_3H	170	0.90	21.2	7.14
Ir/SiO_2–SO_3H	174	0.98	21.8	8.18
Pt/SiO_2–SO_3H	172	0.88	20.5	8.93

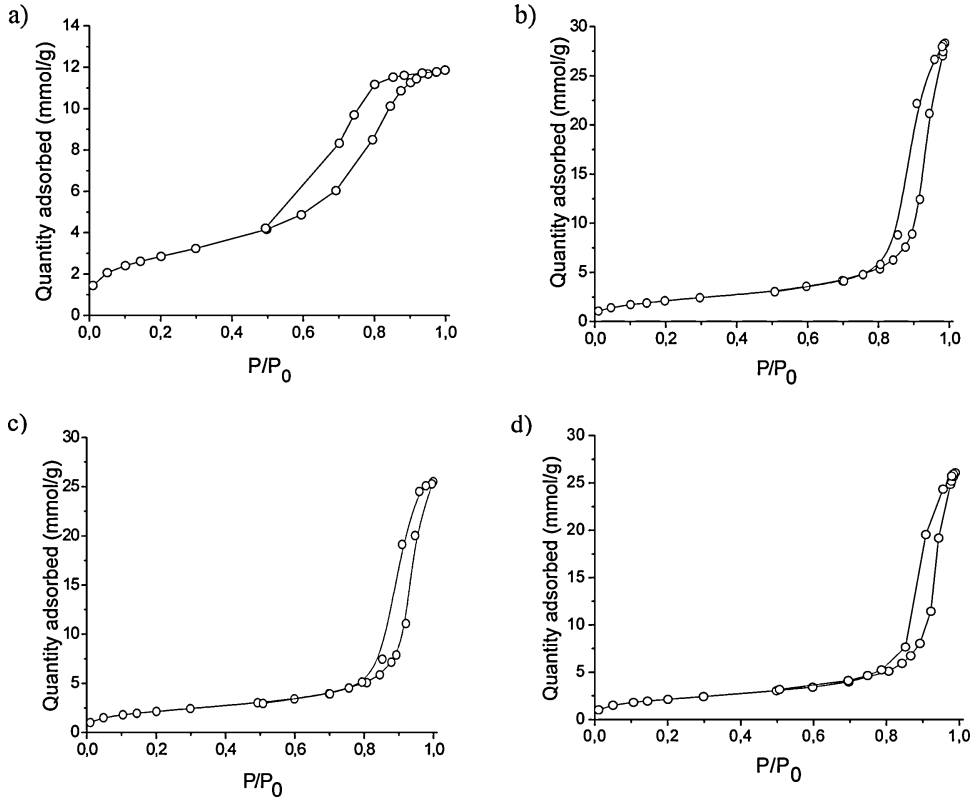

Fig. 2. N_2 physisorption isotherms of (a) SiO_2–SO_3H; (b) Ir/SiO_2–SO_3H; (c) Pt/SiO_2–SO_3H; (d) Au/SiO_2–SO_3H.

colloids with the sulfonic groups. This fact might also explain the increases in the textural properties of Me/SiO_2–SO_3H catalysts.

The XRD patterns of catalysts are shown in Fig. 1. All catalysts exhibit a broad XRD peak assigned to amorphous silica. For Au/SiO_2–SO_3H, signals characteristic of metallic gold ($2\theta = 38.27^\circ$, 44.6°, 64.68° and 77.55°; JCPDS No. 04-0784) are observed. The Pt/SiO_2–SO_3H catalyst shows a signal near $2\theta = 39.67^\circ$ and 46.18° due to the presence of platinum crystallites (JCPDS No. 65-2868), while no reflections were detected for the Ir/SiO_2–SO_3H catalyst. The crystal size of Au and Pt catalysts using the (1 1 1) reflection peaks at $2\theta = 38.27^\circ$ and 39.67° is listed in Table 2.

Table 2
Particle size (d_p) and geometrical dispersion (D) from XRD and the dispersion measured by H_2 chemisorption analysis.

Catalysts	$d_{p\text{-}DRX}$, nm [a]	$D_{(H/Me)}$ [b]	$d_{p\text{-}Quím,nm}$
Au/SiO_2–SO_3H	4.1	n.d.	n.d.
Ir/SiO_2–SO_3H	n.d.	0.53	2.1
Pt/SiO_2–SO_3H	3.7	0.32	3.5

n.d., not determined.
[a] Estimated from XRD results by Debye-Scherrer equation.
[b] Calculated from the results of hydrogen–oxygen titration.

Table 2 tabulates the dispersion ($D_{H/Me}$) and the particle size (d_s) assuming spherical particles calculated from H_2 chemisorption at 308 K. The Au catalyst did not show hydrogen adsorption. The Pt/SiO_2–SO_3H catalyst particle size determined by XRD and H_2-chemisorption analysis was similar.

The surface of the catalysts was characterized by XPS analysis. Fig. 4a–c display XPS spectra in the region of Au, Ir and Pt $4f_{7/2}$ core levels for the metal colloids. The metal 4*f* (Me 4*f*) is characterized by the doublet of two spin–orbit components, viz., Me $4f_{7/2}$ and Me $4f_{5/2}$. In this work, the values of binding energy (BE) will refer to the Me $4f_{7/2}$ peak for comparison with previous reports.

The $Au/SiO_2–SO_3H$ spectrum (Fig. 4 a) shows a binding energy of Au $4f_{7/2}$ at 83.2 eV, which is associated with Au^0 species. Claus et al. [16] found a similar value (BE = 83.28 eV) for Au/SiO_2 catalysts prepared by chemical vapor deposition. However, the reported normal value of Au^0 species is 84.0 eV, and $Au^{\delta-}$ species have lower values [17].

In $Pt/SiO_2–SO_3$, the Pt $4f_{7/2}$ peak was located near 70.1 eV, which could be assigned to zero-valent Pt. Generally, the Pt^0 $4f_{7/2}$ peak is reported at higher binding energy (71.2 eV). The other contributions of Pt $4f_{7/2}$ are at about 70.9 and 72.1 eV, which could probably be associated with Pt(II) and Pt(IV), respectively.

The XPS spectra of $Ir/SiO_2–SO_3$ collected in the region of Ir 4f core level show two contributions to Ir $4f_{7/2}$, namely, at 60.2 eV and 62.5 eV (Fig. 3b). The first contribution should be associated with Ir^0 atoms, while the other should correspond to partially oxidized $Ir^{\delta+}$. As in Pt and Au colloids, the BE of this species is always reported at the highest values [18–21].

An electron transfer does not explain the low binding energy of Au $4f_{7/2}$, Pt $4f_{7/2}$ and Ir $4f_{7/2}$ electrons, since SiO_2 is a nonreducible oxide and in the synthesis method it does not favor an SMSI effect. In this sense, this result should be associated with the particle size, as it is well known that the coordination number of a surface atom is smaller in a nanocluster than in bulk. So, the electron density is larger on the surface of a nanocluster and hence, the binding energy is smaller than in bulk metallic metal [22,23]. However, as the colloids showed distinct particle sizes (XRD results and dispersion measurements), the shifting to a lower binding energy (1.0 eV) on the surface metal atom in Au, Pt and Ir colloids should be explained considering some interaction with the sulfonic groups of the support. Recently, Zhu et al. [12] reported this interaction between the sulfonic groups and Ru nanoparticles in $Ru/SiO_2–SO_3H$ catalysts; the electron transfer between the sulfonic groups and Ru nanoparticles was evidenced as a shift to lower binding energy values. Thus, this fact should be taken into account for explaining the results in metallic colloids supported on $SiO_2–SO_3H$.

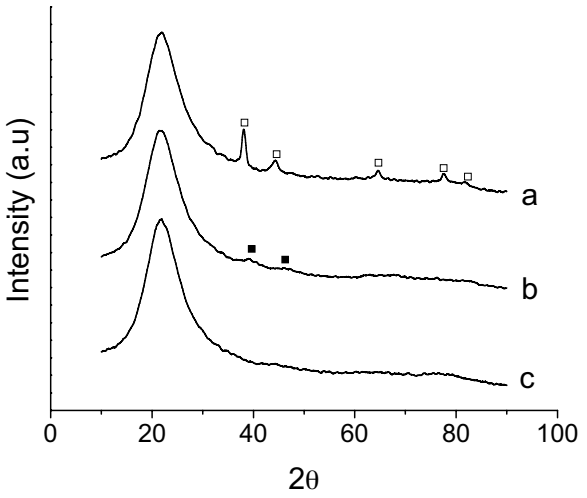

Fig. 3. X-ray patterns of supported Au catalysts: (a) $Au/SiO_2–SO_3H$, (b) $Pt/SiO_2–SO_3H$, and (c) $Ir/SiO_2–SO_3H$. *Note*: peak assignments: (■) Pt, (□) Au.

3.2. Catalytic activity

The reaction of furfural with aniline in the presence of $Pt/SiO_2–SO_3$ catalyst was chosen as a model reaction for reductive amination studies. In order to optimize the reaction conditions, distinct polar solvents were tested due to the higher yield of the desired product in other reports [10]. Table 3 summarizes the solvent effect on the conversion and yield of the reductive amination

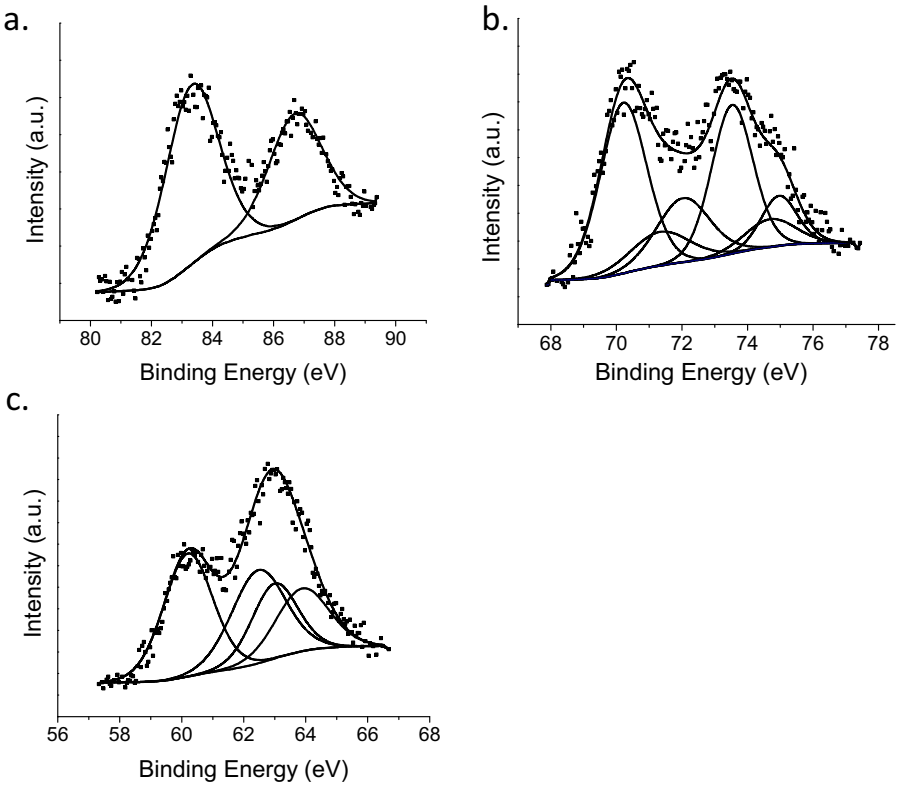

Fig. 4. XPS spectra in the region of Me $4f_{7/2}$ and Me $4f_{5/2}$ of (a) $Au/SiO_2–SO_3H$, (b) $Pt/SiO_2–SO_3H$, and (c) $Ir/SiO_2–SO_3H$.

Table 3
Solvent effect on the reductive amination of furfural with aniline. Reaction conditions: furfural, 6 mmol; aniline, 5 mmol; catalyst, 0.15 mol%; ethyl acetate, 40 mL; H_2 pressure, 5 MPa; and room temperature; time, 8 h.

Solvent	Conversion (%)[a]	Yield to imine (%)	Yield to amine (%)
Methanol	46	41.4	5.1
Water	24	13.2	11.3
Ethyl acetate	72	51.2	21.3
THF	69	66.1	14.9

[a] Conversion of aniline determined by GC.

Table 4
Solvent effect on the reductive amination of furfural with aniline. Reaction conditions: furfural, 6 mmol; aniline, 5 mmol; catalyst, 0.15 mol%; ethyl acetate, 40 mL; H_2 pressure, 5 MPa; and room temperature; time, 8 h.

Catalysts	Conversion (%)[a]	Yield to imine (%)	Yield to amine (%)
$Au/SiO_2–SO_3H$	48	45	3
$Ir/SiO_2–SO_3H$	58	38	19
$Pt/SiO_2–SO_3H$	71	50	21

[a] Conversion of aniline determined by GC.

of furfural with aniline. The highest conversion and yield to amine desired was obtained with ethyl acetate.

Lateral reactions were observed mainly due to acid sites with alcoholic solvents. This fact decreases the formation of imine. Thus, methanol reacts rapidly with furfural forming furfuryl acetal, which competes with the formation of imine groups. The formation of acetal was confirmed using the $SiO_2–SO_3H$ support in alcoholic medium, where the formation of imine was also observed.

Although water is an environmentally benign, safe, and inexpensive solvent, a high reversibility in the formation of imine, as well as the formation of a hydroxylamine derivate, occurs.

In THF solvent condensation products were observed, while ethyl acetate showed the highest amine formation at the reaction conditions set and no side reactions developed. This can be explained considering that ethyl acetate inhibits the formation of imine, due to protonation of aniline (decreased nucleophilicity, lower yield to imine). However, in THF aniline would not be protonated and would be available to act as a nucleophile (highest yield to imine), although the secondary amine formed condenses again, which produces the tertiary imine (other condensation products) following an analogous mechanism for the formation of the secondary amine by-product. With the aim of controlling the selectivity to secondary amine, ethyl acetate was chosen for further optimization studies.

The metal effect was studied using Pt, Ir and Au supported on $SiO_2–SO_3H$ as catalysts. The results are shown in Fig. 5 and Table 4. It is clear that metals such as Ir and Pt favor the hydrogenation step, while the Au catalyst, which poorly dissociates molecular hydrogen, gives the lowest conversion and yield to amine. The low activity of the Au catalyst could be related to the low hydrogen dissociation on gold catalysts [24–26]. The behavior of Ir and Pt catalysts is similar, and the trend is to increase the desired yield to amine with the time of reaction. In this reaction, the yield is not modulated by the nature of the metal, contrary to the results reported by Gomez et al. [11]. This can be explained considering that surfaces grafted with sulfonic groups alter the adsorption of the substrate on the metallic surface, due to the poisoning/coordination of the sulfonic acid group to the metal center [12], which avoids further side reactions favoring the selectivity of the reaction. This type of interaction simultaneously serves to enhance the selectivity and the catalytic activity. Although a slight increase in the yield to amine is observed with the use of Ir catalysts, it is probably due to a smaller particle size [9].

In order to analyze the effect of the sulfonic groups present in SiO_2, Pt/SiO_2 catalysts prepared by colloidal method and a typical procedure of impregnation were compared (Fig. 6). In the Pt/SiO_2 catalysts, where there are no $-SO_3H$ sites, amine formation is not favored. The reaction proceeds slowly without the acidic sites, however in $Pt/SiO_2–SO_3H$, acid sites favors the hydrogenation of the imine and consequently, the desired amine formation. Besides, the results of XPS demonstrate the interaction between the sulfonic group and metal nanoparticles, which suppose that the hydrogenation step of imine to amine should occur in sites close to $Me–SO_3H$.

When only the support was used as catalyst, the only product observed was imine, suggesting the requirement of the metal for the reduction of imine. The formation of imine mainly over the acid support emphasizes the importance of Pt in reducing the imine formed on the $-SO_3H$ sites of the catalyst. Thus, it seems that the presence of acid sites favors acid catalysis of imine homogeneous equilibrium.

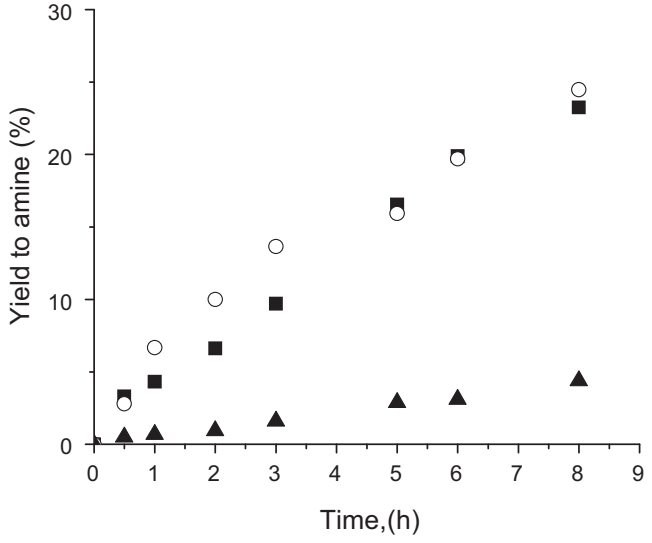

Fig. 5. Effect of the metal employed on furfural amination. (○) $Ir/SiO_2–SO_3H$, (■) $Pt/SiO_2–SO_3H$ (▲) $Au/SiO_2–SO_3H$. Reaction conditions: furfural, 6 mmol; aniline, 5 mmol; catalyst, 0.15 mol %; ethyl acetate, 40 mL; H_2 pressure, 5 MPa; room temperature; time, 8 h.

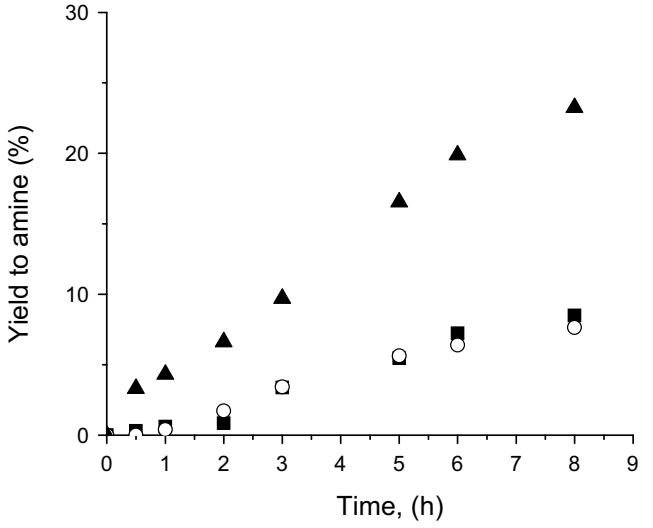

Fig. 6. Effect of the presence of sulfonic groups grafted on SiO_2: (○) Pt/SiO_2 prepared by impregnation of Pt colloidal, (■) Pt/SiO_2 prepared by conventional impregnation (▲) $Pt/SiO_2–SO_3H$ prepared by impregnation of Pt colloidal. Reaction conditions: furfural, 6 mmol; aniline, 5 mmol; catalyst, 0.15 mol%; ethyl acetate, 40 mL; H_2 pressure, 5 MPa; room temperature; time, 8 h.

4. Conclusions

Reductive amination proceeds slowly without the acidic sites; however, the interaction of SO_3H sites favors the formation of imine and its subsequent hydrogenation to amine, being possible to control the yield to amine with ethyl acetate. The interaction of sulfonic groups with metallic particles was demonstrated by the shift to lower BE in the XPS analysis. This shift was clearly observed in all the metallic colloids prepared. The order of activity in the reductive amination of furfural with aniline was Pt ≈ Ir > Au, and the selectivity to amine was not affected by the type of metal employed since the Me–SO_3H interaction avoided further side reactions, favoring the catalytic activity.

Acknowledgment

We thank DIN-UPTC for the financial support under project No. SGI 1281.

References

[1] A. Heydari, S. Khaksar, J. Akbari, M. Esfandyari, M. Pourayoubi, M. Tajbakhsh, Tetrahedron Lett. 48 (2007) 1135–1138.
[2] R.S. Varma, R. Dahiya, Tetrahedron 54 (1998) 6293–6298.
[3] P.S. Reddy, S. Kanjilal, S. Sunitha, R.B.N. Prasad, Tetrahedron Lett. 48 (2007) 8807–8810.
[4] H. Alinezhad, Z. Tollabian, Bull. Korean Chem. Soc. 31 (2010) 1927–1930.
[5] H. Alinezhad, M. Tajbakhsh, M. Zare, Synth. Commun. 39 (2009) 2907–2916.
[6] J. Deng, L.-P. Mo, F.-Y. Zhao, L.-L. Hou, L. Yang, Z.-H. Zhang, Green Chem. 13 (2011) 2576–2584.
[7] A. Srivani, P.S.S. Prasad, N. Lingaiah, Catal. Lett. 142 (2012) 389–396.
[8] Annemieke W. Heinen, Joop A. Peters, Herman v. Bekkum, Eur. J. Org. Chem. 2000 (2000) 2501–2506.
[9] M.E. Domine, M.C. Hernández-Soto, M.T. Navarro, Y. Pérez, Catal. Today 172 (2011) 13–20.
[10] D.B. Bagal, R.A. Watile, M.V. Khedkar, K.P. Dhake, B.M. Bhanage, Catal. Sci. Technol. 2 (2012) 354–358.
[11] S. Gomez, J. Peters, J. van der Waal, W. Zhou, T. Maschmeyer, Catal. Lett. 84 (2002) 1–5.
[12] W. Zhu, H. Yang, J. Chen, C. Chen, L. Guo, H. Gan, X. Zhao, Z. Hou, Green Chem 16 (2014) 1534–1542.
[13] F.W. Lichtenthaler, Ullmann's Encyclopedia of Industrial Chemistry, Wiley-VCH Verlag GmbH & Co. KGaA, Weinheim, 2000.
[14] W. Yu, M. Liu, H. Liu, J. Zheng, J. Colloid Inter. Sci. 210 (1999) 218–221.
[15] M.L. Testa, V. La Parola, L.F. Liotta, A.M. Venezia, J. Mol. Cat. A: Chem. 367 (2013) 69–76.
[16] J. Radnik, C. Mohr, P. Claus, Phys. Chem. Chem. Phys. 5 (2003) 172–177.
[17] J.J. Martínez, H. Rojas, L. Vargas, C. Parra, M.H. Brijaldo, F.B. Passos, J. Mol. Cat. A: Chem. 383–384 (2014) 31–37.
[18] P. Reyes, M.C. Aguirre, I. Melián-Cabrera, M. López Granados, J.L.G. Fierro, J. Catal. 208 (2002) 229–237.
[19] W. Lin, H. Cheng, L. He, Y. Yu, F. Zhao, J. Catal. 303 (2013) 110–116.
[20] H. Rojas, G. Borda, P. Reyes, J.J. Martínez, J. Valencia, J.L.G. Fierro, Catal. Today 133–135 (2008) 699–705.
[21] J.J. Martínez, G. Borda, P. Reyes, H. Rojas, Catalysis of Organic Reactions, CRC Press, Boca Raton, FL, 2008, pp. 117–125.
[22] S. Arrii, F. Morfin, A.J. Renouprez, J.L. Rousset, J. Am. Chem. Soc. 126 (2004) 1199–1205.
[23] F. Somodi, I. Borbáth, M. Hegedűs, A. Tompos, I.E. Sajó, Á. Szegedi, S. Rojas, J.L.G. Fierro, J.L. Margitfalvi, Appl. Catal. A: Gen. 347 (2008) 216–222.
[24] R. Zanella, C. Louis, S. Giorgio, R. Touroude, J. Catal. 223 (2004) 328–339.
[25] T. Fujitani, I. Nakamura, T. Akita, M. Okumura, M. Haruta, Angew. Chem. Int. Ed. Engl. 48 (2009) 9515–9518.
[26] E. Bus, J.A. Van Bokhoven, Phys. Chem. Chem. Phys. 9 (2007) 2894–2902.